DINAME 2019 - Proceedings of the XVIII International Symposium on Dynamic Problems of Mechanics,
M.A. Savi, T.G. Ritto and W.M. Bessa (Editors), ABCM, Buzios, RJ, Brazil, March 10th to 15th, 2019

Active Modal Control Applying in a 2DOF Structure

Joana Pereira Repinaldo[1] , Edson Hideki Koroishi[1] , Fabian Andres Lara Molina[1] , Aldemir Ap Cavalini Jr[2] and Valder Steffen Jr[2]

[1] Federal University of Technology-Paraná, Campus Cornélio Procópio, Av. Alberto Carazzai, 1640, ZIP CODE 86300-000, Cornélio Procópio-PR, Brazil.

[2] LMEst - Structural Mechanics Laboratory, Federal University of Uberlândia, School of Mechanical Engineering, Av. João Naves de Ávila, 2121, ZIP CODE 38408-144, Uberlândia, MG, Brazil.

Abstract: This paper proposes an active modal control technique through electromagnetic actuators, which is applied to a structure with two degrees of freedom. To develop an effective control, it is necessary to build mathematical models capable of accurately representing the dynamic behavior of the mechanical system. The experimental characterization of the mechanical system of two degrees of freedom consists in identifying the unknown parameters through the solution of an inverse problem by using the optimization technique namely differential evolution. From the estimated parameters, it is possible to apply the active modal control to the system. The modal control was used since it allows the control of the vibration amplitude corresponding to a specific mode shape. The control was based on two different approaches. The first one is based on the neuro-fuzzy modal control and the second is based on the fuzzy logic approach. In the experimental tests, a state observer was included to estimate the modal states of the system. Numerical and experimental results demonstrate the effectiveness of the adopted control strategies considering the reduction of the vibration amplitudes.

Keywords: active modal control, neuro-fuzzy modal, fuzzy modal.

INTRODUCTION

Undesired oscillations may occur in structures when subjected to dynamic forces. Different control methods are used to minimize these oscillations. Active vibration control applies secondary forces in the structure by using various types of actuators (Zang et al., 2016). Among the active control methods, the modal control technique demonstrated to be an interesting approach in previous applications. The modal control is based on a transformation from physical to modal space. Modal controllers can be designed by using various techniques, such as the fuzzy logic. The architecture of control based on fuzzy logic does not require the mathematical model of the system to be controlled. The human experience and expertise to implement the fuzzy controller through linguistic terms are used instead (Gomide and Pedrycz, 2006). However, the accuracy of the fuzzy control is associated with the effective determination of these linguistic terms. The fuzzy controller can be adapted by modifying its parameters and employing learning techniques (Pourzeynali et al., 2007). Systems that have integrated artificial neural networks with fuzzy logic are called neuro-fuzzy systems, which incorporate the advantages of artificial intelligence, such as its capability of learning, with the advantages of fuzzy systems.

In the present contribution, the experimental tests were performed in a mechanical system with two DoFs. The unknown parameters of the system were determined by comparing experimental and simulated frequency response functions (FRFs). In this sense, the optimization algorithm known as differential evolution was used. Finally, the dynamic response of the system containing fuzzy and neuro-fuzzy modal controllers were evaluated both numerically and experimentally.

Structure Identification

The analyzed structure is represented by a system of two degrees of freedom that is represented by Eq. (1):

$$[m]\{\ddot{d}(t)\}+[c]\{\dot{d}(t)\}+[k]\{d(t)\}=\{f(t)\} \tag{1}$$

where $[m]$, $[k]$, and $[c]$ are the mass, stiffness, and damping matrices, respectively, $\{f(t)\}$ is the force vector, and $\{d(t)\}$ is the displacement vector.

The identification of the unknown parameters of the two DoFs structure (i.e., stiffness and damping coefficients) was performed by solving a typical inverse problem, which consists of minimizing the difference between numerical and experimental FRFs by using the above mentioned optimization technique.

The acquisition system showed in Fig. 1 was used to obtain the experimental FRFs. The Data Physics Quattro® acquisition board measures the excitation force applied to the system by using an impact hammer and the corresponding

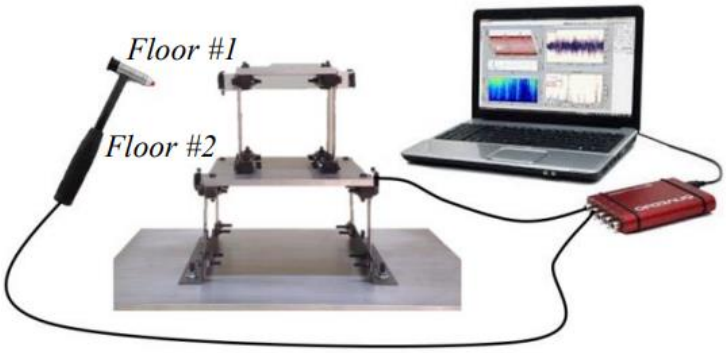

Figure 1 – Identification data acquisition system.

vibration responses are measured by using an accelerometer. The input and output signals were treated through the software SignalCalc ACE®. This procedure was performed sequentially involving five tests to obtain average values for the FRFs. In this case, four FRFs were obtained by performing impacts and measuring the vibration responses along the floors #1 and #2 (see Fig. 1).

The differential evolution optimization algorithm (Viana, 2008) was applied by considering a different number of individuals in the initial population: 50, 100,150, and 200. The unknown parameters and associated design intervals adopted in the optimization problem are shown in Tab. 1. Figure 2 shows the comparison between the experimental FRFs.

Table 1 – Design space adopted in the optimization process.

Parameters	Design Space
Stiffness $k_{floor\#1}$ [N/m]	$9000 \le k_1 \le 40000$
Damping $c_{floor\#1}$ [N.s/m]	$0 \le c_1 \le 25$
Stiffness $k_{floor\#2}$ [N/m]	$8000 \le k_2 \le 20000$
Damping $c_{floor\#2}$ [N.s/m]	$0 \le c_2 \le 10$

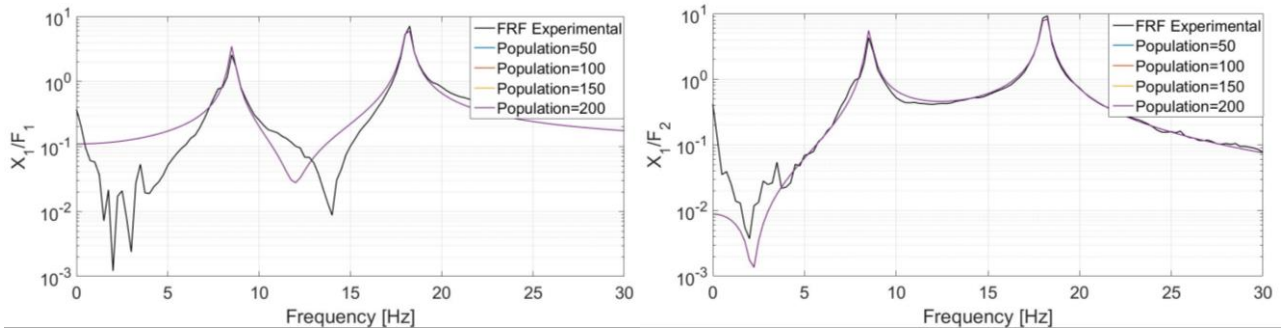

a)

b)

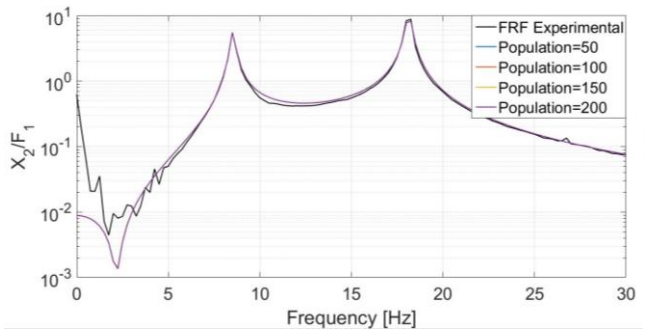

c)

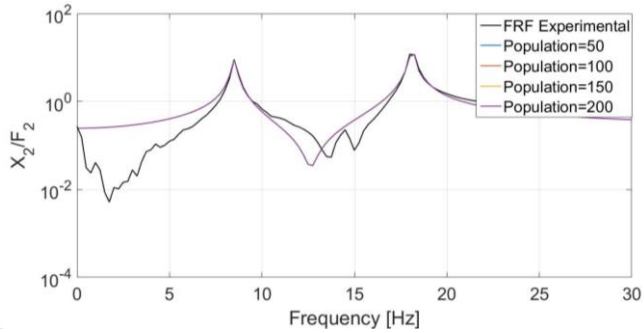

d)

Figure 2 – Experimental and identified FRFs: a) impact at floor #1 and measurement of floor #1; b) impact at floor #1 and measurement of floor #2; c) impact at floor #2 and measurement of floor #1; d) impact in floor #2 and measurement of floor #2.

Figure 2 shows the comparison between the experimental and simulated FRFs for the corresponding number of individuals in the initial population of the optimization problem. Note that there is a small variability on the identified FRFs according to the number of individuals used in the initial population of the optimizer. Additionally, the numerical and experimental FRFs are similar, thus demonstrating the representativeness of the identified model. It can be observed that the stiffness and damping parameters used are those obtained for the population of 50 individuals. The parameters of the system are shown in Tab. 2.

Table 2 – Parameters obtained in the optimization.

Parameters	Value
Mass m_1 [kg]	4.38
Stiffness k_1 [N/m]	$2.15x10^4$
Damping c_1 [N.s/m]	14.43
Mass m_2 [kg]	1.94
Stiffness k_2 [N/m]	$3.18x10^{-8}$
Damping c_2 [N.s/m]	0.622

Control Approach

An active control approach was applied to the two DoFs structure through the fuzzy and neuro-fuzzy modal controllers, in which an electromagnetic actuator provided the control effort. A state observer was used to estimate the modal states of the system. Figure 3 shows the controller scheme. In this case, both *Fuzzy 1* and *Neuro-Fuzzy 1* controllers were designed aiming to attenuate the vibration amplitude of the first vibration mode of the structure. *Fuzzy 2* and *Neuro-Fuzzy 2* controllers are devoted to the second vibration mode of the structure.

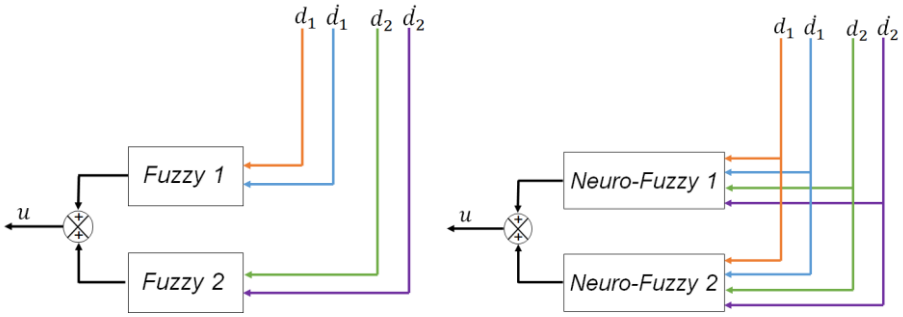

Figure 3 – Modal controllers.

Figure 4 shows the experimental setup and the control strategy adopted in the present contribution, where F_{exc} is

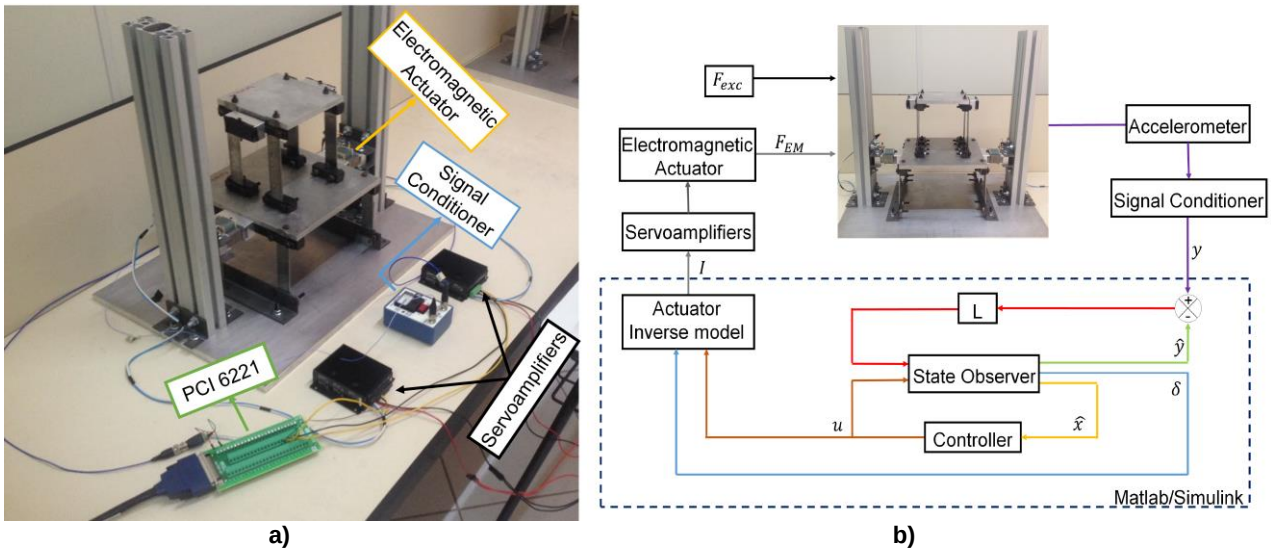

a) **b)**

Figure 4 – a) Experimental control and acquisition system; b) control strategy.

the excitation force applied in the system, F_{em}, is the actuator control force, y is the output vector, $\hat{x}$ is the estimated state vector, $\hat{y}$ is the estimated output vector, and δ is the displacement of the controlled floor (*Floor #1*). In this case, an accelerometer is used to measure the vibration responses of the structure. The National Instruments® acquisition system PCI-6621 and the software Matlab/Simulink® were used to perform the control.

Pole placement

The pole placement method consists of determining a state feedback gain, so that the poles of the closed-loop system are placed at any desired locations (Ogata, 2013). Considering the feedback control given by Eq. (2):

$$\{\dot{x}(t)\} = [A]\{x(t)\} + [B]\{u(t)\} \tag{2}$$

where $[A]$ is the dynamic matrix, $[B]$ is the input matrix, $\{x(t)\}$ is the state vector, and $\{u(t)\}$ is the input force. Substituting in Eq. (2) the signal of state feedback control as given by $\{u(t)\} = -[G]\{x(t)\}$:

$$\{\dot{x}(t)\} = ([A] - [B][G])\{x(t)\} \tag{3}$$

The gain $[G]$ can be determined by using the Ackermann's formula. Thus:

$$[G] = [0 \quad 0 \quad \dots \quad 0 \quad 1] * [B \ \vdots \ AB \ \vdots \ \dots \ \vdots \ A^{n-1}B]^{-1} * \phi A \tag{4}$$

where ϕA is given by Eq (5).

$$\phi A = A^n + \alpha_1 A^{n-1} + \cdots + \alpha_{n-1} A + \alpha_n I = 0 \tag{5}$$

Fuzzy Logic

The Fuzzy Inference System is composed of the following components: fuzzification, knowledge base, inference engine, and defuzzification. In the fuzzification, two membership *gbell* functions are used, as given by Eq (6).

$$\mu_i(z) = \frac{1}{1 + \left| \dfrac{x(t) - P}{L} \right|^{2H}} \tag{6}$$

where L, H, and P are the parameters of the *gbell* function. Figure 5 shows the degree of membership of the *gbell* function for the input values.

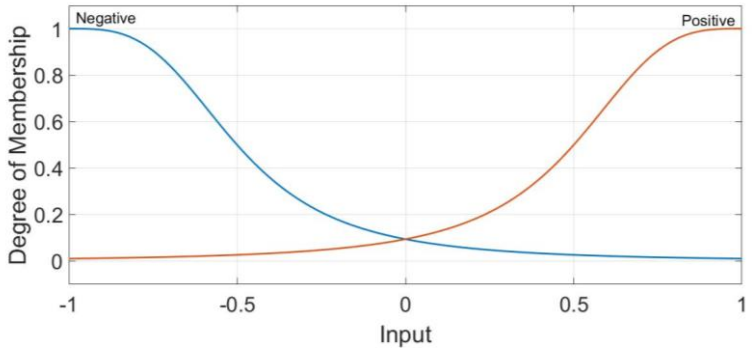

Figure 5 – Fuzzy membership function.

The controller rules are presented in Tab. 3 and Tab. 4, where four rules were created in the conditional statement (If-then) for each controller. The inference engine adopted was Takagi-Sugeno, with output values presented in Eq (7).

$$z_1 = 0, \ z_2 = \begin{bmatrix} -112.8 & 40.7 & 0 \end{bmatrix}\{x\} \text{ and } z_3 = \begin{bmatrix} -51.85 & 40.92 & 0 \end{bmatrix}\{x\} \tag{7}$$

Neuro-Fuzzy

The Neuro-Fuzzy structure was chosen as based on the architecture developed by Jang (1993), called Adaptive Neuro-Fuzzy Inference System (ANFIS). The neuro-fuzzy modal control uses the optimized parameters of the

Table 3– Fuzzy 1 controller rules.

Rules	x_1	$\dot{x}_1$	Output
1	Positive	Positive	z_2
2	Positive	Negative	z_1
3	Negative	Positive	z_1
4	Negative	Negative	z_2

Table 4– Fuzzy 2 controller rules.

Rules	x_2	$\dot{x}_2$	Output
1	Positive	Positive	z_3
2	Positive	Negative	z_1
3	Negative	Positive	z_1
4	Negative	Negative	z_3

fuzzy controller by using a neural network approach, in which the objective function is the learning of the desired input-output pairs. For simplicity, the ANFIS architecture considered two inputs, X and Y, and an output Z, as illustrated in Fig. 6.

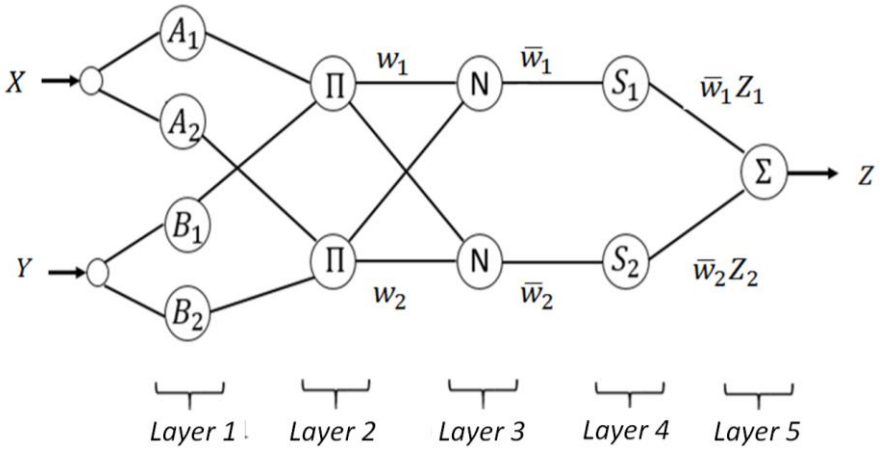

Figure 6 – ANFIS architecture.

In *layer 1*, the membership degree of the inputs X and Y is calculated, as given by Eq (8).

$$\mu_{Ai}(X), \mu_{Bi}(Y), i = 1,2, \tag{8}$$

In *layer 2*, each node output represents the degree of applicability of a rule, resulting in Eq (9).

$$w_i = \mu_{Ai}(X) \times \mu_{Bi}(Y), i = 1,2. \tag{9}$$

In *layer 3*,the normalized membership functions are performed. In this layer, the ratio of the *i-th* rule's applicability with respect to the sum of all rules' firing strengths is calculated, as given by Eq (10).

$$\overline{w}_i = \frac{w_i}{w_1 + w_2}, i = 1,2. \tag{10}$$

In *layer 4*, the parameters are given by Eq (11). The values of p_i, q_i, and r_i correspond to constants to be adjusted in the training process.

$$Z_1 = p_1 X + q_1 Y + r_1, \; Z_2 = p_2 X + q_2 Y + r_2 \tag{11}$$

In *layer 5*, there is the defuzzification of the signals that compute the overall output as the sum of all incoming signals, as given by Eq (12).

$$\sum_i \overline{w}_i Z_i = \frac{\sum_i w_i Z_i}{\sum_i w_i}, i = 1,2. \tag{12}$$

The parameters of each layer are updated according to the training data and the learning process. The hybrid-learning algorithm combines the recursive least-squares estimation method and the backpropagation gradient descent technique.

The Neuro-Fuzzy control was modeled by using the Toolbox ANFIS of Matlab/Simulink®. The same parameters presented for the Fuzzy controller were optimized for the Neuro-Fuzzy controller. The architecture of the neural network used in the present work is depicted in Fig. 7.

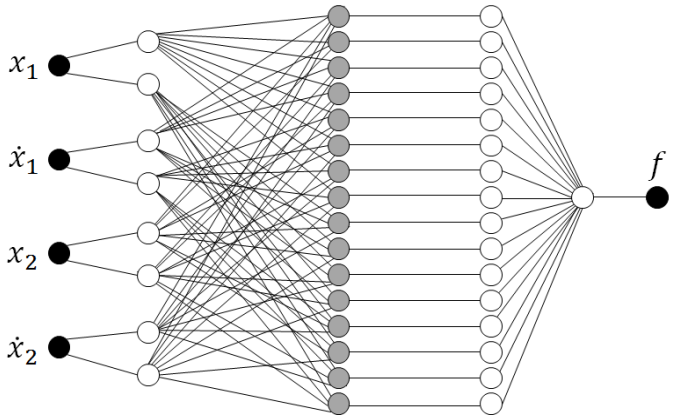

Figure 7 – Neural Network.

The network of neurons has the function of learning based on the desired input-output set. Then, pole placement was performed as the training base for the Neuro-Fuzzy control. The gain of the controller (pole placement) was defined by varying the damping coefficients ξ_1 and ξ_2. Two control gains were used for training the Neuro-Fuzzy controller, being one for the first vibration mode (*Neuro-Fuzzy 1*) of the structure and another for the second vibration mode (*Neuro-Fuzzy 2*).

Figure 8 illustrates the responses of the feedback control as obtained by pole placement. This is performed by varying the damping coefficient ξ_1. Note that the amplitude of the first natural frequency decreases as ξ_1 increases. However, by increasing the damping coefficient results a spillover condition at the second natural frequency. Figure 8b shows that the vibration amplitude decreases as ξ_1 increases. However, it can be observed that the vibration component associated with the second vibration mode appears in the vibration responses for values of ξ_1 close to its critical value.

Similar analysis was applied for the second vibration mode of the system by varying ξ_2 (see Fig. 9). In this case, spillover is observed for the first natural frequency as ξ_2 increases. The time domain vibration responses according to ξ_2 are illustrated in Fig. 9b.

The damping coefficients ξ_1 = 0.05 and ξ_2 = 0.0078 were used to obtain the training data training data for the Neuro-Fuzzy 1 controller. Note that ξ_1 = 0.05 reduced the vibration amplitude of the first vibration mode without

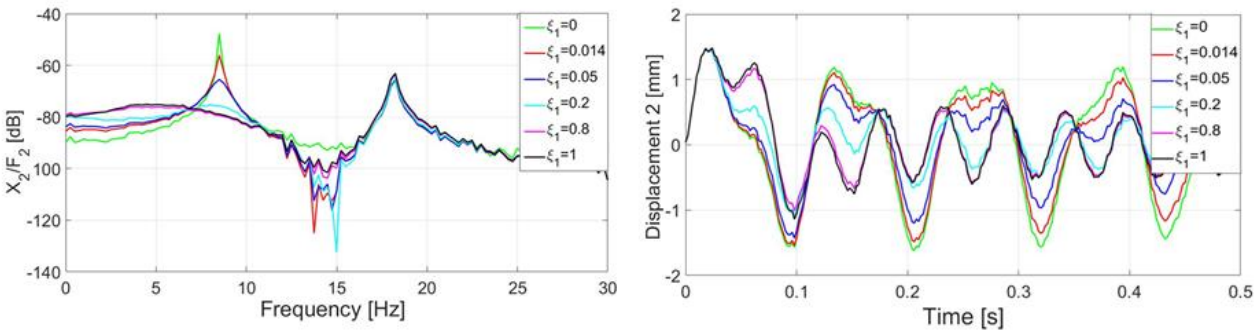

a) **b)**

Figure 8 – a) Simulated FRFs; b) simulated impact response.

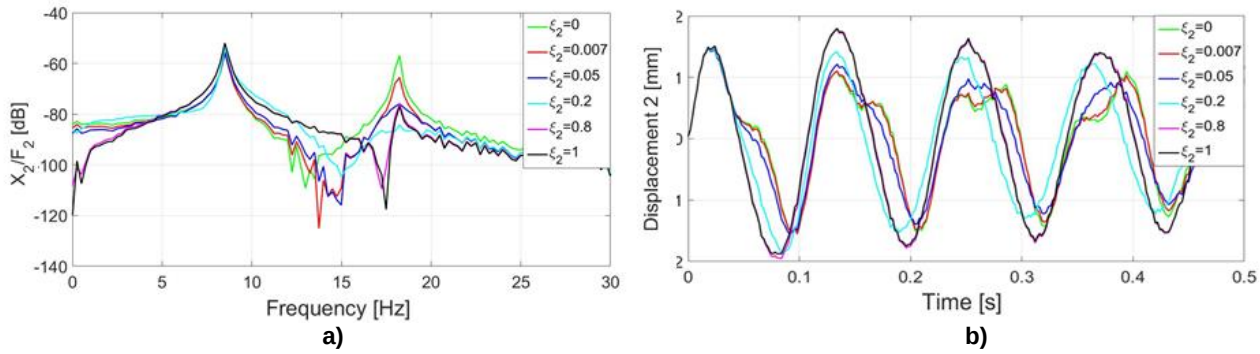

Figure 9 – a) Simulated impact response for different values of ξ_2 ; b) simulated FRFs for ξ_2 .

increasing the spillover in the second mode. The training base of the *Neuro-Fuzzy 2* controller presented the same criteria used for the *Neuro-Fuzzy 1* controller. Therefore, the damping coefficients were ξ_1 = 0.015 and ξ_2 = 0.03.

For the ANFIS training, the input parameters were the following: error tolerance equal to zero, hybrid training, and 100 training epochs. Figure 10 shows the degree of membership obtained after the training of the *Neuro-Fuzzy1* control and Fig. 11 shows the results associated with the *Neuro-Fuzzy2* controller.

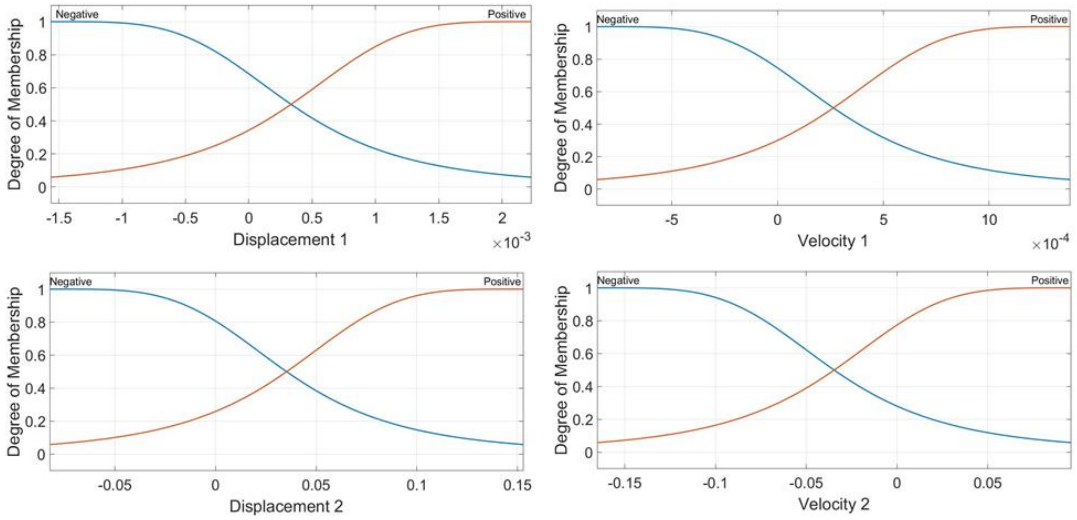

Figure 10 – Membership function *Neuro-Fuzzy1*.

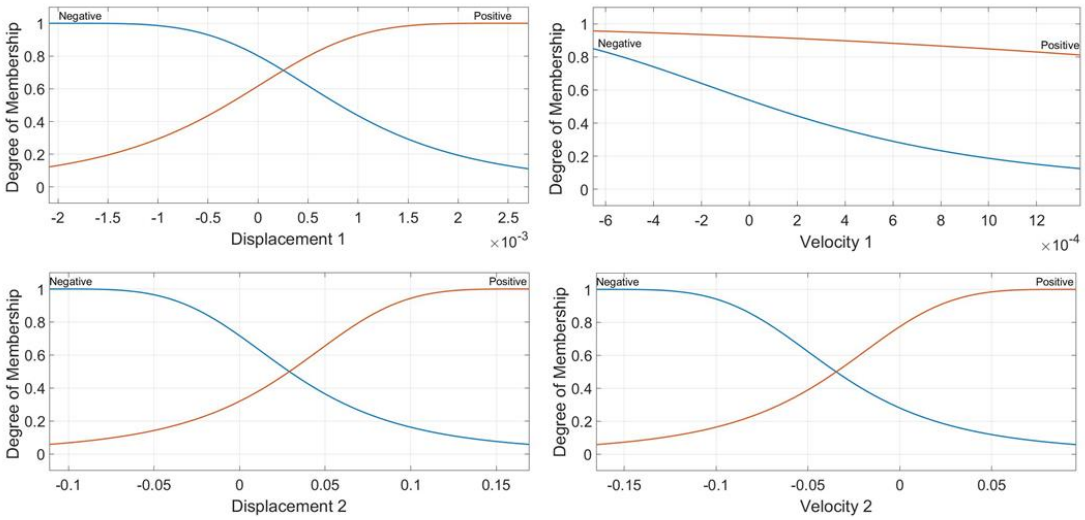

Figure 11 – Membership function *Neuro-Fuzzy2*.

The rules of the controllers are presented in Tab. 5, where sixteen rules have been created in the conditional statement *If-then* for each controller. The inference engine adopted was the Takagi-Sugeno's, with output values presented in Eq (13), where α_i, β_i, γ_i, and λ_i are different for each output z_i.

$$z_i = [\alpha_i \quad \beta_i \quad \gamma_i \quad \lambda_i]\{s\} \tag{13}$$

Table 5 – Neuro-Fuzzy controller rules.

Rules	x_1	$\dot{x}_1$	x_2	$\dot{x}_2$	Output
1	Positive	Positive	Positive	Positive	z_2
2	Positive	Positive	Positive	Negative	z_1
3	Positive	Positive	Negative	Positive	z_2
4	Positive	Positive	Negative	Negative	z_1
5	Positive	Negative	Positive	Positive	z_1
6	Positive	Negative	Positive	Negative	z_1
7	Positive	Negative	Negative	Positive	z_1
8	Positive	Negative	Negative	Negative	z_1
9	Negative	Positive	Positive	Positive	z_1
10	Negative	Positive	Positive	Negative	z_1
11	Negative	Positive	Negative	Positive	z_1
12	Negative	Positive	Negative	Negative	z_1
13	Negative	Negative	Positive	Positive	z_2
14	Negative	Negative	Positive	Negative	z_1
15	Negative	Negative	Negative	Positive	z_1
16	Negative	Negative	Negative	Negative	z_2

Electromagnetic Actuator

In this work, electromagnetic actuators are used to apply the control forces for active vibration control purposes. The parameters of the actuators are shown in Tab. 6. An inverse model of the electromagnetic actuators is used to determine the electric current required to obtain the control forces, as given by Eq. (14).

Table 6 – Parameters of the actuators.

Parameters	**Value**
μ_o [H/m]	4π x 10^{-7}
N	237
a [mm]	9.5
b [mm]	38
c [mm]	28.5
d [mm]	9.5
f [mm]	21.5
e [mm]	2
μ_r	688.27

$$I = \sqrt{\frac{2F_{em}\left((e \pm \delta) + \dfrac{b+c+d-2a}{\mu_r}\right)^2}{N^2 \mu_o a f}} \tag{14}$$

where the parameters a, b, c, d , and f define the geometry of the solenoid, μ_r and μ_o are the magnetic permeability and vacuum permeability, respectively, N is the number of turns, e is the gap, and δ corresponds to the displacement.

RESULTS

Figure 12 presents the simulated results obtained for the controlled structure when an impact force is applied at the *Floor #2*. The results demonstrate the effectiveness of both control approaches to attenuate the vibration amplitudes of the structure. The amplitude attenuation was obtained for a time smaller than 1 sec for the Neuro-Fuzzy controller and 1.5 s for the Fuzzy controller. Figure 12b shows a significant reduction in the amplitudes of both peaks of the FRF obtained by applying an impact force at the *Floor #2* and performing the response at *Floor #2*. Note that the amplitude of the two vibration modes were attenuated 6.78 dB by using the fuzzy controller and 9.42 dB by using the neuro-fuzzy controller for the first natural frequency and 5.56 dB by using the fuzzy controller and 8.76 dB by using the neuro-fuzzy controller for the second natural frequency. Despite high attenuation of the response was achieved by using the Neuro-Fuzzy controller, the simulations demonstrated high-energy consumption of the actuators as compared with the Fuzzy controller. The control efforts applied by the actuators are presented in Fig. 13.

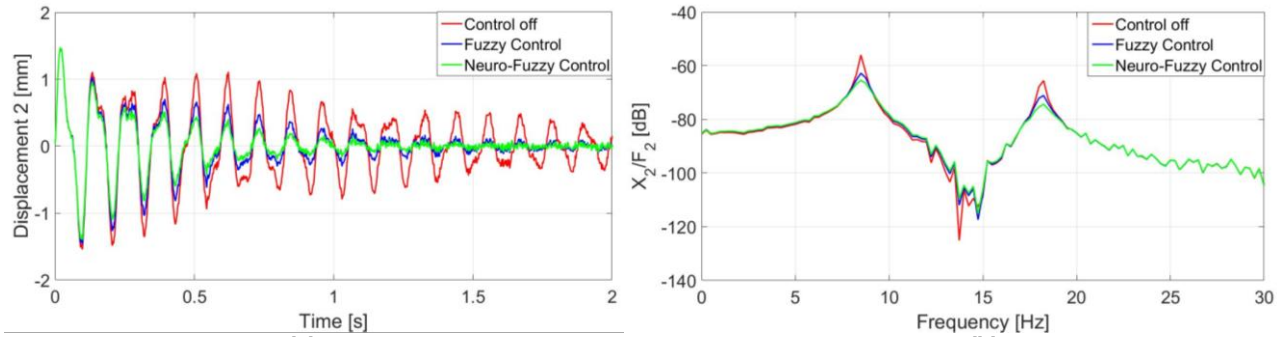

Figure 12 – a) Simulated impact response; b) simulated FRFs.

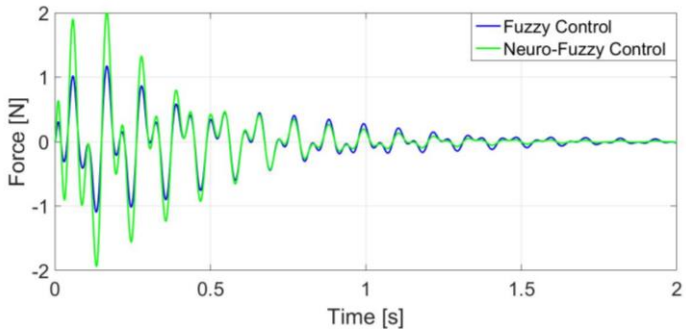

Figure 13 – Simulated control effort.

Figure 14 presents the experimental results. The control effort was applied to the structure by the electromagnetic actuator located at the *Floor #1*. Regarding the impact response (see Fig. 14a), the attenuation time of the oscillations was smaller than 1.5 sec. The FRFs of the system with and without control are depicted in Fig. 14b. Note that both the controllers are able to attenuate the amplitude of the two natural frequencies of the system, namely 7.48dB for the Fuzzy control and 8.90dB for the Neuro-Fuzzy control for the first natural frequency and 7.63dB for the Fuzzy control and 10.14dB for the Neuro-Fuzzy control for the second natural frequency. Figure 15 shows the experimental control effort for the two types of controllers.

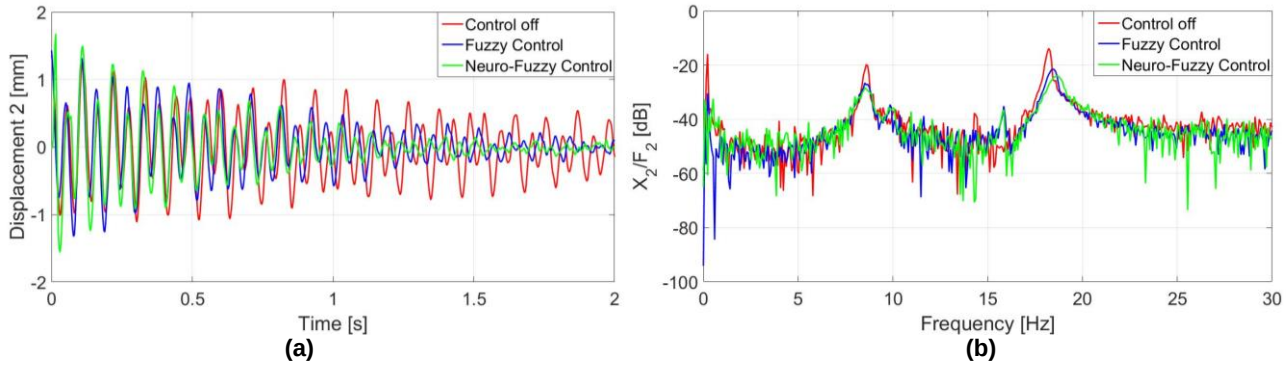

Figure 14 – a) Experimental impact response; b) experimental FRFs.

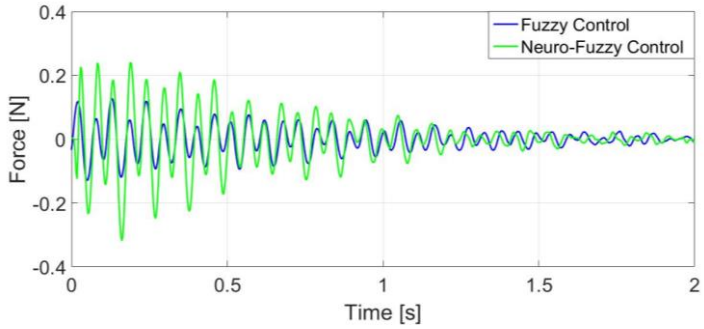

Figure 15 – Experimental control effort.

CONCLUSION

The obtained results demonstrated the efficiency of the identification methodology to determine the unknown parameters of the 2 DoFs system. The identification of the parameters performed by using the differential evolution technique allowed the characterization of the structure and the model representativeness required by the considered active modal controllers. The numerical and experimental results demonstrated that both designed controllers were efficient to attenuate the vibration responses of the system by using electromagnetic actuators. In general, experimental results are in good agreement with the simulations. The differences between the simulations and experiments since the second natural frequency increases with the control application. The neuro-fuzzy controller showed better results as compared to the fuzzy controller.

ACKNOWLEDGMENTS

The authors gratefully acknowledge the financial support for this research from CNPq (Process 402581/2016-4), Araucária Foundation and CAPES.

REFERENCES

Gomide, F.A.C., Pedrycz, W., 2006, “An Introduction to Fuzzy Sets: Analysis and Design”, Ed. Bradford, Boston, 465 p.

Jang, J. S. R. ,1993, “ANFIS: adaptive-network-based fuzzy inference system”, IEEE Transactions on Systems, Man, and Cybernetics, Vol.23, n.3.

Ogata, K., 2013, “Engenharia de Controle Moderno”,Ed. Prentice Hall, São Paulo, 894p.

Pourzeynali, S., Lavasani, H.H., Modarayi, A.H., 2007, “Active Control of High Rise Building Structures using Fuzzy Logic and Genetic Algorithms”, Engineering Structures, Vol.29, pp. 346-357.

Viana, F.A.C., 2008, “Surrogate modeling techniques and heuristic optimization methods applied to design and identification problems”, Tese (Doutorado) Universidade Federal de Uberlândia, Uberlândia.

Zhang, P., Mills, A., Zambreno, J., Jones, P.H., 2017, “The Design and Integration of a Software Configurable And Parallelized Coprocessor Architecture for LQR Control”, Journal of Parallel and Distributed Computing, Vol.106, pp. 121-131.

RESPONSIBILITY NOTICE

The authors are the only responsible for the printed material included in this paper.